University of Bath

1
2
3
4
5
6
7
8
9
10
11
12

Photon-pair generation in photonic crystal fibre with a 1.5 GHz modelocked VECSEL

Oliver J. Morris[a,1], Robert J. A. Francis-Jones[b,1], Keith G. Wilcox[a,c], Anne C. Tropper[a], Peter J. Mosley[b]

[a]*School of Physics and Astronomy, University of Southampton, Southampton, SO17 1BJ, UK*
[b]*Centre for Photonics and Photonic Materials, Department of Physics, University of Bath, Bath, BA2 7AY, UK*
[c]*Division of Engineering, Physics and Mathematics, University of Dundee, Nethergate, Dundee, DD1 4HN*

Abstract

Four-wave mixing (FWM) in optical fibre is a leading technique for generating high-quality photon pairs. We report the generation of photon pairs by spontaneous FWM in photonic crystal fibre pumped by a 1.5 GHz repetition-rate vertical-external-cavity surface-emitting laser (VECSEL). The photon pairs exhibit high count rates and a coincidence-to-accidental ratio of over 80. The VECSEL's high repetition-rate, high average power, tunability, and small footprint make this an attractive source for quantum key distribution and photonic quantum-state engineering.

Keywords: single photon; photon pair; VECSEL; four-wave mixing.

1. Introduction

The drive towards photonic quantum-enhanced technologies is placing ever more stringent demands on the performance of nonclassical light sources [1–3]. However due to their size, cost, complexity, and limited generation rates it is challenging to incorporate state-of-the-art photon sources into turn-key systems. Nevertheless in recent years, huge advances have been made in producing higher-quality single photons from straightforward equipment operating at room temperature. Optical nonlinearity has been at the forefront of these efforts [4–10].

By propagating a high-intensity laser pulse through a nonlinear medium, pairs of photons can be spontaneously generated, either through parametric downconversion (PDC), a three-wave mixing process that requires the presence of $\chi^{(2)}$ nonlinearity, or by $\chi^{(3)}$-mediated four-wave mixing (FWM). The

---

highest-performance sources are usually pumped by Ti:Sapphire oscillators [11–16], placing them orders of magnitude higher in both complexity and cost than the attenuated laser sources typically used in commercially-available quantum technologies. Furthermore, the repetition rate of these lasers, usually 80 MHz or so, places a limit on the rate at which high-quality photon pairs can be delivered by a single source [17]. These factors present significant obstacles to implementing real-world photonic quantum-enhanced technologies.

In this paper we demonstrate photon-pair generation through four-wave mixing in a photonic crystal fibre (PCF) driven by a 1.5 GHz modelocked tunable vertical-external-cavity surface-emitting laser (VECSEL) [18]. VECSELs have not previously been used for photon-pair generation but are attractive for a number of reasons [19]. Modelocked VECSELs produce transform-limited ultrafast pulses with peak power in the correct range for photon-pair generation by FWM in fibre [20]. Modelocking a VECSEL requires a compact cavity containing only three or four components providing the possibility of very small-footprint photon-pair sources that require little maintenance. The short cavity results in a high pulse repetition frequency which could allow an order of magnitude increase in the rate of pair generation relative to 80 MHz laser systems. VECSELs are intrinsically flexible: the wavelength can be continuously tuned by an intracavity etalon [18]; the repetition rate can be adjusted without interrupting modelocking by translating the output coupler [21]; and the wavelength range and pulse duration (and hence the spectral bandwidth) can be changed by using different semiconductor substrates. Such flexibility gives great scope for optical quantum-state engineering, as discussed towards the end of this paper.

2. Four-wave mixing in photonic crystal fibre

Photon-pair generation by degenerate FWM involves the annihilation of two photons and the corresponding creation of a photon pair, known as the signal and idler, at equal frequency detunings above and below the pump. All that is required is a material providing $\chi^{(3)}$ nonlinearity and sufficient peak power to access the nonlinearity; hence the process is usually pumped by high-power laser pulses. While the strength of the $\chi^{(3)}$ nonlinearity is orders of magnitude smaller than that available in the equivalent $\chi^{(2)}$ pair generation process – PDC – the ubiquity of the $\chi^{(3)}$ nonlinearity makes photon-pair generation by spontaneous FWM possible in optical fibre, where long interaction lengths are available. This also has the advantage of generating photon pairs in a well-defined guided mode, ensuring efficient collection and straightforward interfacing with subsequent fibre components or waveguiding optical chips [22–24].

FWM in photonic crystal fibre (PCF) is ideally placed to exploit the properties of VECSELs. Unlike many semiconductor lasers, the external cavity endows VECSELs with exceptional beam quality allowing efficient coupling into the fundamental mode of a fibre. The long interaction length and small mode area in fibre means that the peak power required for photon-pair generation is relatively low; indeed, if the peak power is too high parasitic nonlinear effects such as Raman scattering will dominate and degrade the quality of the quantum

states produced. The high repetition rate of a modelocked VECSEL means that even at large average powers the pulse energy is small ($\sim 500\,\text{pJ}$) and the peak power commensurately low, which helps to limit unwanted nonlinear effects. Finally, the dispersion of PCF can be modified during fabrication by selecting the dimensions of the photonic crystal cladding; coupled with the flexibility in bandwidth and wavelength tunability of VECSELs this gives significant control over the properties of the generated photon pairs.

When FWM is pumped by a single laser pulse (the degenerate pump case) and all fields are co-polarised and propagate in the fundamental mode of a fibre, the phasematching conditions that govern the generation of photon pairs can be written

$$2\omega_\text{p} - \omega_\text{s} - \omega_\text{i} = 0 \tag{1}$$

$$2k_\text{p} - k_\text{s} - k_\text{i} - 2\gamma P_0 = 0 \tag{2}$$

where angular frequencies $\omega_\text{p,s,i}$ and wavenumbers $k_\text{p,s,i}$ correspond to the pump, signal, and idler respectively. γ is the nonlinearity of the fibre and P_0 the peak power of the pump. The resulting quantum state is correlated in photon number but dominated by the vacuum component; it can be written:

$$|\Psi_\text{FWM}\rangle \propto |0_\text{s}, 0_\text{i}\rangle + \lambda|1_\text{s}, 1_\text{i}\rangle + \lambda^2|2_\text{s}, 2_\text{i}\rangle + \cdots \tag{3}$$

where λ is proportional to P_0 and the generation probability for n pairs is $P(n) \propto |\lambda|^{2n}$ [25, 26]. The $|0_\text{s}, 0_\text{i}\rangle$ term is usually eliminated by heralding (detecting one photon to announce the presence of the other) or post-selecting on a successful generation event.

In order to generate high-quality photon pairs, we wish to maximise the contribution from the $|1_\text{s}, 1_\text{i}\rangle$ component in Equation 3 and minimise the higher-order terms [27]. It is clear from Equation 3 that although increasing λ by turning up the peak power P_0 will yield a higher pair generation rate, it will also increase the emission rate of two or more pairs simultaneously. This rapidly degrades the quality of the photon-pair source. As a result, sources are usually limited to $\lambda \ll 1$ so that the pair generation probability per pulse is below 1%, limiting the total number of pairs that can be generated per second.

Changing the pump laser repetition rate can reconcile these conflicting demands [28]. Increasing the repetition rate by a factor m reduces the peak power to P_0/m and therefore $\lambda \to \lambda/m$, leading to a reduction of order m^2 in the relative contribution of multiple-pair emission compared to singe-pair generation. Although reducing the peak power at constant average power also reduces the rate of single pairs generated by FWM by a factor of m, pulsed FWM sources are anyway forced to operate far below the maximum average power that the pump laser is capable of delivering. Hence the single-pair generation rate can be restored by increasing the average pump power, and the ratio of two-pair to one-pair generation events will still be reduced by a factor of m. Conversely, if the pair generation probability per pulse is kept constant, increasing the repetition rate allows the pair generation rate to increase by the same factor m without any impact on the ratio of two-pair to one-pair generation events.

3

3. Vertical-external-cavity surface-emitting laser

The VECSEL, shown schematically in Figure 1, is an optically pumped, semiconductor quantum-well laser. The gain chip of the laser, fabricated by NAsP III/V GmbH (Marburg, Germany), was epitaxially grown on top of a $500\,\mu$m thick GaAs substrate. It consisted of an InGaP cap layer, a $12\lambda/2$ thick GaAsP active region containing 11 InGaAs quantum wells and a 22-pair AlGaAs/AlAs distributed Bragg reflector (DBR) in this order. Solid-liquid inter-diffusion bonding was used to place a diamond heat spreader in direct thermal contact with the DBR and a chemical etch was applied to remove the substrate. The structure was then mounted diamond side down on a water-cooled copper heat-sink maintained at 18 °C.
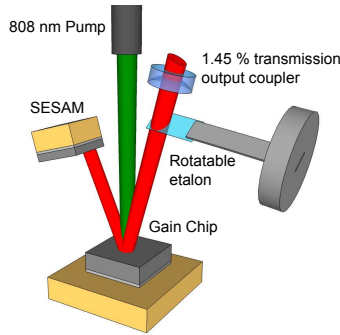

Figure 1: Schematic of the laser cavity. See text for details.

The VECSEL was modelocked by incorporating a Semiconductor Saturable Absorber Mirror (SESAM) into the cavity. The SESAM structure used in this work was provided by BATOP optoelectronics (SAM-1064-0.7-1ps) and had a modulation depth of 0.4 %, a non-saturable loss of 0.3 %, a saturation fluence of $130\,\mu$J/cm^2 and a damage threshold of $3\,$mJ/cm^2. The cavity was completed with a 1.45 % transmission, $100\,$mm radius of curvature (ROC) output coupler.

Pump light is absorbed by the quantum well spacer layers creating carriers that become localised within the quantum wells. An $808\,$nm fibre-coupled diode laser was used to pump the gain chip with $23\,$W of light focused to a $125\,\mu$m radius spot. In order to match the absorption of the SESAM to the emission of the gain chip, the SESAM was cooled to -10°C using a Peltier-cooled heat-sink.

The external cavity formed by the free-standing output coupler and SESAM allows the insertion of intracavity elements. An uncoated $25\,\mu$m-thick fused silica etalon was placed into the VECSEL cavity between the output coupler and the gain chip and held close to the Brewster angle of the s-polarised laser mode. The thickness of the etalon equates to a free spectral range (FSR) at normal incidence of $14\,$nm. The incorporation of the etalon both stabilised the mode-locked operation and, by rotating the etalon about the Brewster angle, provided $\pm4.5\,$nm of wavelength selectivity around a centre wavelength of $1027\,$nm.

(a) Autocorrelation

(b) Optical Spectrum

(c) RF Spectrum (1st Harmonic)

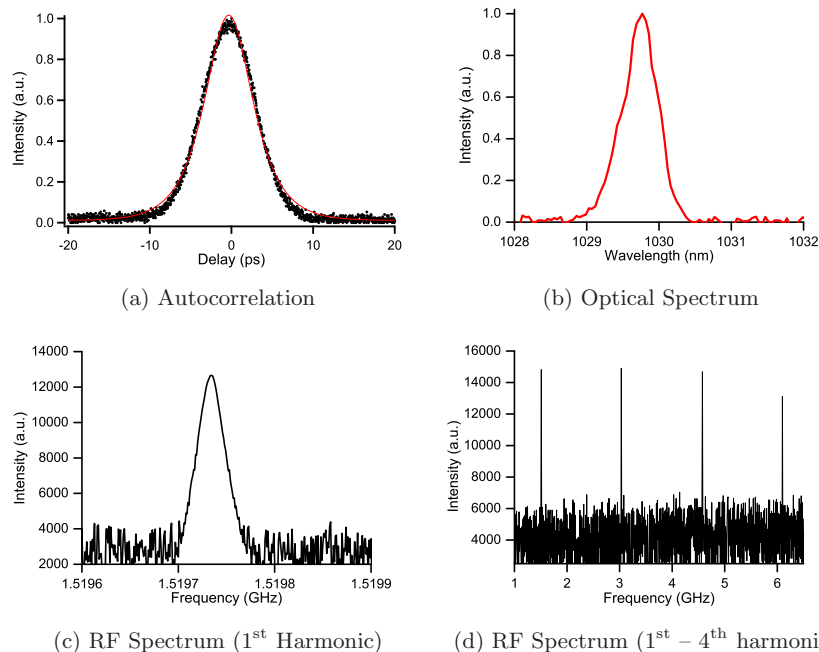(d) RF Spectrum (1st − 4th harmonics)

Figure 2: Characterisation of 4.5 ps modelocked VECSEL source emitting 1 W of average power at 1030 nm: (2a) Autocorrelation corresponding to a pulse duration of 4.5 ps. (2b) Optical spectrum corresponding to a centre wavelength of 1029.8 nm. (2c) RF spectrum of the 1st harmonic corresponding to a repetition rate of 1.5 GHz. (2d) RF spectrum of the first four harmonics.

Performance data are shown in Figure 2. The VECSEL emitted 4.5 ps pulses at a repetition rate of 1.5 GHz, and was optimised for operation around 1030 nm. The average output power was 1 W corresponding to a peak power of 140 W.

4. GHz repetition-rate photon-pair source

We have built a source of photon pairs based on the tunable VECSEL reported above and a PCF fabricated in Bath by the stack-and-draw technique. The PCF used in the experiments reported here was formed of a solid silica glass core surrounded by a cladding region formed by a triangular array of air holes in a silica glass matrix. The hole spacing (pitch) was approximately 3 μm and the ratio of hole diameter to pitch was approximately 0.4. Its zero-dispersion wavelength was measured using white-light interferometry to be at 1058 nm and a simulated dispersion profile based on these parameters is shown in Figure 3 [29]. Using a PCF with bespoke dispersion allowed us to generate

5

signal photons around 800 nm where silicon detectors have high efficiency and idler photons within the low-loss window of conventional telecomms fibre around 1550 nm.
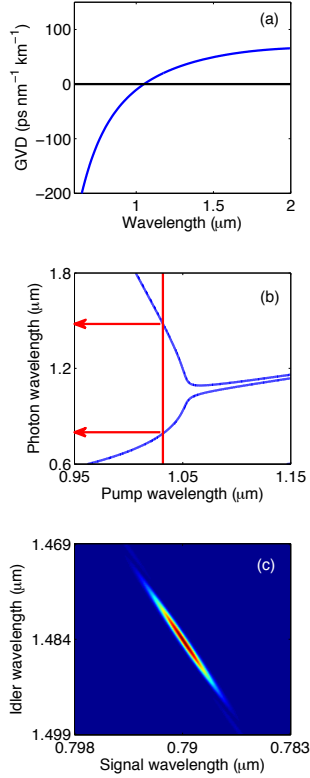

Figure 3: (a) Modelled PCF group-velocity dispersion (GVD) and (b) corresponding FWM phasematching. (c) shows a calculated probability density plot for the resulting two-photon state when pumped at 1029 nm.

The photon-pair source is shown in Figure 4. The beam from the VEC-SEL was cleaned by two long-wave-pass filters to remove any residual 808 nm light originating in the pump diodes, and passed through two half-wave plates separated by a polarising beamsplitter for power and polarisation control. The VECSEL pulses were monitored continuously via pick-off beams directed to a spectrometer and an autocorrelator.

The pump pulses were coupled into and out of the PCF using aspheric lenses. Following the PCF, a half-wave plate and polariser selected only light co-polarised with the pump. The signal and idler were split with a dichroic mirror and the residual 1029 nm pump was removed from both arms with additional
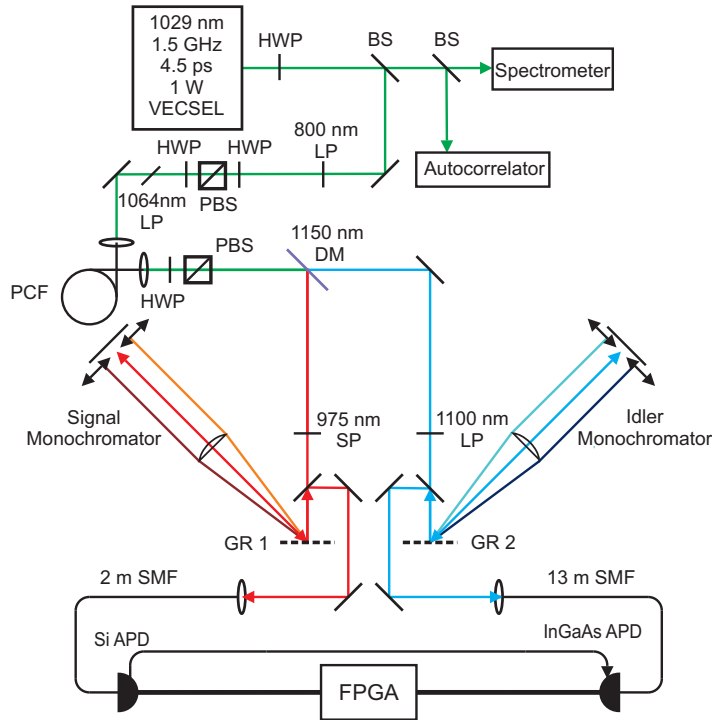
Figure 4: VECSEL-pumped photon-pair source. See text for details.

interference filters. Subsequently both signal and idler passed through home-built grating monochromators to reduce any remaining background from the 808 nm VECSEL pump diodes, 1029 nm pulses, or spontaneous Raman scattering into the long-wavelength arm [30] and allow measurement of the signal and idler wavelengths. The photons were then coupled into conventional single-mode fibre (SMF-28 in the idler arm and SM800 in the signal arm).

Using CW diode lasers at 780 nm and 1550 nm we measured the total transmission from the output face of the PCF to the outputs of the single-mode fibres. We found over 90% loss within the transmission bands of each arm, including all filtering and coupling. Approximately half of this loss originates in the grating monochromators, with the remaining half dominated by coupling into the single-mode fibres. The matching of the guided mode in the PCF to the two single-mode fibres was hampered by the chromatic variation in focal length of the aspheric lens after the PCF; as a result it was necessary to compromise between good coupling in the long- and short-wavelength arms. Loss from the other components following the PCF was negligible.

The 800 nm photons were routed through 2 m of SM800 to a free-running silicon avalanche photodiode (Perkin-Elmer SPCM). An InGaAs detector (idQuan-

tique id201) was used to monitor the 1550 nm arm. It could not be operated in free-running mode and had a maximum gate frequency of 1 MHz – over three orders of magnitude lower than the repetition frequency of the pump laser. Therefore the output pulses from the Si APD were used to gate the InGaAs APD. The 1550 nm photons were delayed in 13 m of fibre to provide sufficient time for the InGaAs detector to become active before the corresponding photon arrived. The count rates from both detectors were monitored by a home-built field-programmable gate array (FPGA) coincidence counting unit.

Figure 5 shows a typical plot of the InGaAs detector count rate as a function of the internal delay between the arrival of the trigger pulse and the detection window opening. With the delay set to 7.5 ns, the detection window of the InGaAs APD encompassed the arrival times of photons generated by the same pump pulse as those detected at the Si APD. The height of this peak therefore showed the number of coincidence counts per second between the signal and idler arms. Away from this peak is a constant background level of accidental coincidence events arising from uncorrelated generation and detection processes. The ratio of coincidence counts to accidental background events is known as the coincidence-to-accidentals ratio or CAR and is a strong indicator of source performance.
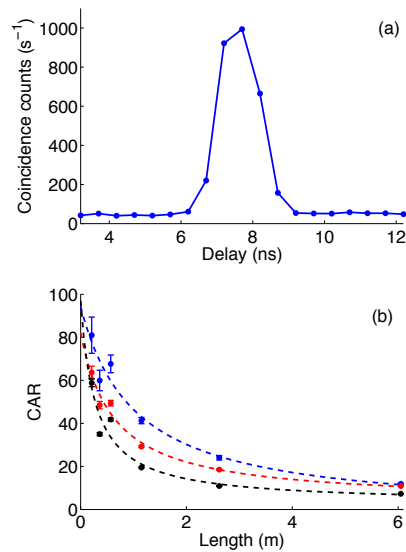

Figure 5: (a) A typical plot of InGaAs APD count rates (equal to the coincidence count rate) against internal detector delay. (b) Coincidence-to-accidental ratio as a function of PCF length for average pump powers of 50 mW (blue), 100 mW (red), and 150 mW (black). Dotted lines are fits proportional to $1/L$.

The gate width of the InGaAs APD was set to its minimum value of 2.5 ns.

Because the detection events at the Si APD were used to trigger the InGaAs detector, any photons arriving within the gate of the InGaAs detector were registered as coincidence counts and the width of the coincidence peak was set by the detector gate width. It can be seen from Figure 5 that the resulting effective coincidence window is less than 2 ns, or approximately three times the laser repetition period. Therefore for each detection event at the Si APD there were three possible pump pulses within which any corresponding photons counted by the InGaAs APD could have originated. Nevertheless, the high-contrast coincidence signal at 7.5 ns and constant background at all other delays is strong evidence of a correlated generation process from a single pump pulse as one would expect from FWM. Within the limitations of the detectors available, there was no possibility of reducing the coincidence window to a single pump pulse, however suitable avalanche photodiodes have been gated at over 2 GHz [31].

With the pump wavelength set to 1029 nm, the central wavelengths and bandwidths of the monochromators were adjusted to maximise the CAR. The central wavelengths of signal and idler were found to be approximately 780 nm and 1515 nm respectively.

In order to optimise the length of the PCF in the photon-pair source, we began with a 6 m length of PCF and cut it back while monitoring the CAR. The results for three different power levels are shown in Figure 5. It can be seen that the CAR was reasonably high at all times, never dropping below 7. The CAR rose rapidly as the PCF length was reduced below 1 m indicating a significant improvement in source performance; the highest measured value of the CAR was over 80, using 50 mW average pump power and a PCF length of 210 mm, and at an absolute coincidence count rate of almost 1000 pairs/s. This fibre length corresponded to approximately half the calculated walk-off length between the signal and idler and the 4.5 ps pump pulses (450 mm and 340 mm respectively).

The absolute count rates were limited by the high level of loss following the PCF, particularly in the idler arm. Nevertheless the highest recorded coincidence count rate was 9600 pairs/s with a CAR of 19 from 150 mW average pump power in a fibre length of 1.15 m. Subtracting the measured accidental coincidence rate (480/s) and taking into account the loss after the PCF of over 90% in each arm and detection efficiencies of 60% (signal) and 25% (idler) implies a pair generation rate of at least 6×10^6 pairs/s and a generated brightness of over 4×10^4 pairs/s/mW within bandwidths of approximately 4 nm in the signal arm and 6 nm in the idler.

In future, we expect to be able to reduce the loss and significantly increase the absolute count rates by moving to an all-fibre spliced system, thereby extending the source performance far beyond this proof-of-principle demonstration.

5. Additional capabilities – tuning and state engineering

With the PCF reported above, tuning the VECSEL over its full range of 1027 ± 4.5 nm would allow generation of photon pairs from 751 – 790 nm (1600

– 1484 nm) for the signal (idler). More significantly than this, the tunability and bandwidth of the VECSEL can be exploited for for quantum state engineering – controlling the properties of the photon pairs and heralded single photons through modification of the fibre dispersion [32]. The one-pair component of the state that results from FWM can be written

$$|1_s, 1_i\rangle = |\psi(\omega_s, \omega_i)\rangle = \int_{-\infty}^{\infty} d\omega_s d\omega_i f(\omega_s, \omega_i)|\omega_s, \omega_i\rangle, \qquad (4)$$

where $f(\omega_s, \omega_i)$ is the two-photon amplitude or joint spectrum. In general this amplitude contains correlation between the signal and idler in both the frequency and time domains. The correlation arises because the photons are created together in a parametric process subject to energy and momentum conservation. As a result, detecting each photon yields distinguishing information about its twin, projecting the remaining heralded single photons into mixed quantum states that are largely useless for information-processing tasks.

In order to herald single photons in pure quantum states the photon-pair amplitude must be uncorrelated [33]. Producing an uncorrelated two-photon state is not trivial, and there are two critical requirements: control of the material dispersion and sufficient pump bandwidth to ensure that energy conservation does not dominate the joint state [34–38]. The VECSEL has enough bandwidth, and, while we can fabricate PCF with a wide range of different dispersion profiles, fine control of the dispersion is a major challenge. Even a small degree of of tunability in the pump laser is hugely beneficial to compensate for small errors in fabrication and allow the precise phasematching requirements to be accessed.

6. Conclusion

FWM in PCF is an attractive method for producing photon pairs for quantum-information applications, as it combines the simplicity of nonlinear wave-mixing techniques with guided-wave architecture to allow high-efficiency pair generation. We have demonstrated a new combination of ultra-high repetition-rate VECSEL and PCF that provides new possibilities in reducing detrimental multiple-pair emission while maintaining good count rates and a very high CAR. The small footprint and simplicity of the laser are attractive for integration while its bandwidth and tunability, in conjunction with the flexible dispersion offered by PCF, make it amenable to photonic quantum-state engineering.

7. Acknowledgements

References

[1] J. L. O'Brien, A. Furusawa, J. Vuckovic, Photonic quantum technologies, Nat Photon 3 (12) (2009) 687–695.
URL http://dx.doi.org/10.1038/nphoton.2009.229

[2] M. D. Eisaman, J. Fan, A. Migdall, S. V. Polyakov, Single-photon sources and detectors, Review of Scientific Instruments 82 (7) (2011) 071101. doi:10.1063/1.3610677.
URL http://link.aip.org/link/?RSI/82/071101/1

[3] J.-W. Pan, Z.-B. Chen, C.-Y. Lu, H. Weinfurter, A. Zeilinger, M. Żukowski, Multiphoton entanglement and interferometry, Rev. Mod. Phys. 84 (2012) 777–838. doi:10.1103/RevModPhys.84.777.
URL http://link.aps.org/doi/10.1103/RevModPhys.84.777

[4] C. Söller, B. Brecht, P. J. Mosley, L. Y. Zang, A. Podlipensky, N. Y. Joly, P. S. J. Russell, C. Silberhorn, Bridging visible and telecom wavelengths with a single-mode broadband photon pair source, Phys. Rev. A 81 (3) (2010) 031801. doi:10.1103/PhysRevA.81.031801.

[5] C. Xiong, C. Monat, A. S. Clark, C. Grillet, G. D. Marshall, M. J. Steel, J. Li, L. O'Faolain, T. F. Krauss, J. G. Rarity, B. J. Eggleton, Slow-light Enhanced Correlated Photon-Pair Generation in Silicon, ArXiv e-printsarXiv:1106.3593.

[6] M. J. Collins, A. S. Clark, J. He, D.-Y. Choi, R. J. Williams, A. C. Judge, S. J. Madden, M. J. Withford, M. J. Steel, B. Luther-Davies, C. Xiong, B. J. Eggleton, Low raman-noise correlated photon-pair generation in a dispersion-engineered chalcogenide as2s3 planar waveguide, Opt. Lett. 37 (16) (2012) 3393–3395. doi:10.1364/OL.37.003393.
URL http://ol.osa.org/abstract.cfm?URI=ol-37-16-3393

[7] F. Steinlechner, P. Trojek, M. Jofre, H. Weier, D. Perez, T. Jennewein, R. Ursin, J. Rarity, M. W. Mitchell, J. P. Torres, H. Weinfurter, V. Pruneri, A high-brightness source of polarization-entangled photons optimized for applications in free space, Opt. Express 20 (9) (2012) 9640–9649. doi:10.1364/OE.20.009640.
URL http://www.opticsexpress.org/abstract.cfm?URI=oe-20-9-9640

[8] M. Karpiński, C. Radzewicz, K. Banaszek, Dispersion-based control of modal characteristics for parametric down-conversion in a multimode waveguide, Opt. Lett. 37 (5) (2012) 878–880. doi:10.1364/OL.37.000878.
URL http://ol.osa.org/abstract.cfm?URI=ol-37-5-878

[9] E. Pomarico, B. Sanguinetti, T. Guerreiro, R. Thew, H. Zbinden, Mhz rate and efficient synchronous heralding of single photons at telecom wavelengths, Opt. Express 20 (21) (2012) 23846–23855. doi:10.1364/OE.20.023846.
URL http://www.opticsexpress.org/abstract.cfm?URI=oe-20-21-23846

11

[10] A. R. McMillan, L. Labont, A. S. Clark, B. Bell, O. Alibart, A. Martin, W. J. Wadsworth, S. Tanzilli, J. G. Rarity, Two-photon interference between disparate sources for quantum networking, Sci. Rep. 3.
URL http://dx.doi.org/10.1038/srep02032

[11] P. J. Mosley, J. S. Lundeen, B. J. Smith, P. Wasylczyk, A. B. U'Ren, C. Silberhorn, I. A. Walmsley, Heralded generation of ultrafast single photons in pure quantum states, Physical Review Letters 100 (13) (2008) 133601. doi:10.1103/PhysRevLett.100.133601.
URL http://link.aps.org/abstract/PRL/v100/e133601

[12] A. Ling, J. Chen, J. Fan, A. Migdall, Mode expansion and bragg filtering for a high-fidelity fiber-based photon-pair source, Opt. Express 17 (23) (2009) 21302–21312. doi:10.1364/OE.17.021302.
URL http://www.opticsexpress.org/abstract.cfm?URI=oe-17-23-21302

[13] A. Eckstein, A. Christ, P. J. Mosley, C. Silberhorn, Highly efficient single-pass source of pulsed single-mode twin beams of light, Phys. Rev. Lett. 106 (1) (2011) 013603. doi:10.1103/PhysRevLett.106.013603.

[14] A. Clark, B. Bell, J. Fulconis, M. M. Halder, B. Cemlyn, O. Alibart, C. Xiong, W. J. Wadsworth, J. G. Rarity, Intrinsically narrowband pair photon generation in microstructured fibres, New Journal of Physics 13 (6) (2011) 065009.
URL http://stacks.iop.org/1367-2630/13/i=6/a=065009

[15] M. Tanida, R. Okamoto, S. Takeuchi, Highly indistinguishable heralded single-photon sources using parametric down conversion, Opt. Express 20 (14) (2012) 15275–15285. doi:10.1364/OE.20.015275.
URL http://www.opticsexpress.org/abstract.cfm?URI=oe-20-14-15275

[16] R.-B. Jin, R. Shimizu, K. Wakui, H. Benichi, M. Sasaki, Widely tunable single photon source with high purity at telecom wavelength, Opt. Express 21 (9) (2013) 10659–10666. doi:10.1364/OE.21.010659.
URL http://www.opticsexpress.org/abstract.cfm?URI=oe-21-9-10659

[17] A. Christ, C. Silberhorn, Limits on the deterministic creation of pure single-photon states using parametric down-conversion, Phys. Rev. A 85 (2012) 023829. doi:10.1103/PhysRevA.85.023829.
URL http://link.aps.org/doi/10.1103/PhysRevA.85.023829

[18] O. J. Morris, K. G. Wilcox, C. R. Head, A. P. Turnbull, P. J. Mosley, A. H. Quarterman, H. J. Kbashi, I. Farrer, H. E. Beere, D. A. Ritchie, A. C. Tropper, A wavelength tunable 2-ps pulse vecsel (2012). doi:10.1117/12.908337.
URL http://dx.doi.org/10.1117/12.908337

[19] A. H. Quarterman, K. G. Wilcox, V. Apostolopoulos, Z. Mihoubi, S. P. Elsmere, I. Farrer, D. A. Ritchie, A. Tropper, A passively mode-locked external-cavity semiconductor laser emitting 60-fs pulses, Nat Photon

12

3 (12) (2009) 729–731.
URL http://dx.doi.org/10.1038/nphoton.2009.216

[20] K. G. Wilcox, A. C. Tropper, H. E. Beere, D. A. Ritchie, B. Kunert, B. Heinen, W. Stolz, 4.35 kw peak power femtosecond pulse mode-locked vecsel for supercontinuum generation, Opt. Express 21 (2) (2013) 1599–1605. doi:10.1364/OE.21.001599.
URL http://www.opticsexpress.org/abstract.cfm?URI=oe-21-2-1599

[21] K. G. Wilcox, A. H. Quarterman, H. E. Beere, D. A. Ritchie, A. C. Tropper, Repetition-frequency-tunable mode-locked surface emitting semiconductor laser between 2.78 and 7.87 ghz, Opt. Express 19 (23) (2011) 23453–23459. doi:10.1364/OE.19.023453.
URL http://www.opticsexpress.org/abstract.cfm?URI=oe-19-23-23453

[22] L. Sansoni, F. Sciarrino, G. Vallone, P. Mataloni, A. Crespi, R. Ramponi, R. Osellame, Two-particle bosonic-fermionic quantum walk via integrated photonics, Phys. Rev. Lett. 108 (2012) 010502. doi:10.1103/PhysRevLett.108.010502.
URL http://link.aps.org/doi/10.1103/PhysRevLett.108.010502

[23] J. B. Spring, B. J. Metcalf, P. C. Humphreys, W. S. Kolthammer, X.-M. Jin, M. Barbieri, A. Datta, N. Thomas-Peter, N. K. Langford, D. Kundys, J. C. Gates, B. J. Smith, P. G. R. Smith, I. A. Walmsley, Boson sampling on a photonic chip, Science 339 (6121) (2013) 798–801. arXiv:http://www.sciencemag.org/content/339/6121/798.full.pdf, doi:10.1126/science.1231692.
URL http://www.sciencemag.org/content/339/6121/798.abstract

[24] M. A. Broome, A. Fedrizzi, S. Rahimi-Keshari, J. Dove, S. Aaronson, T. C. Ralph, A. G. White, Photonic boson sampling in a tunable circuit, Science 339 (6121) (2013) 794–798. arXiv:http://www.sciencemag.org/content/339/6121/794.full.pdf, doi:10.1126/science.1231440.
URL http://www.sciencemag.org/content/339/6121/794.abstract

[25] J. Chen, X. Li, P. Kumar, Two-photon-state generation via four-wave mixing in optical fibers, Phys. Rev. A 72 (2005) 033801. doi:10.1103/PhysRevA.72.033801.
URL http://link.aps.org/doi/10.1103/PhysRevA.72.033801

[26] Q. Lin, F. Yaman, G. P. Agrawal, Photon-pair generation in optical fibers through four-wave mixing: Role of raman scattering and pump polarization, Physical Review A 75 (2) (2007) 023803. doi:10.1103/PhysRevA.75.023803.
URL http://link.aps.org/abstract/PRA/v75/e023803

[27] A. L. Migdall, D. Branning, S. Castelletto, Tailoring single-photon and multiphoton probabilities of a single-photon on-demand source, Phys. Rev.

13

A 66 (2002) 053805. doi:10.1103/PhysRevA.66.053805.
URL http://link.aps.org/doi/10.1103/PhysRevA.66.053805

[28] M. A. Broome, M. P. Almeida, A. Fedrizzi, A. G. White, Reducing multi-photon rates in pulsed down-conversion by temporal multiplexing, Opt. Express 19 (23) (2011) 22698–22708. doi:10.1364/OE.19.022698.
URL http://www.opticsexpress.org/abstract.cfm?URI=oe-19-23-22698

[29] K. Saitoh, M. Koshiba, Empirical relations for simple design of photonic crystal fibers, Opt. Express 13 (1) (2005) 267–274.
URL http://www.opticsexpress.org/abstract.cfm?URI=oe-13-1-267

[30] J. Fulconis, O. Alibart, W. Wadsworth, P. Russell, J. Rarity, High brightness single mode source of correlated photon pairs using a photonic crystal fiber, Opt. Express 13 (2005) 7572–7582.

[31] J. Zhang, P. Eraerds, N. Walenta, C. Barreiro, R. Thew, H. Zbinden, 2.23 ghz gating ingaas/inp single-photon avalanche diode for quantum key distribution (2010). doi:10.1117/12.862118.
URL http://dx.doi.org/10.1117/12.862118

[32] K. Garay-Palmett, H. J. McGuinness, O. Cohen, J. S. Lundeen, R. Rangel-Rojo, A. B. U'ren, M. G. Raymer, C. J. McKinstrie, S. Radic, I. A. Walmsley, Photon pair-state preparation with tailored spectral properties by spontaneous four-wave mixing in photonic-crystal fiber, Opt. Express 15 (22) (2007) 14870–14886.
URL http://www.opticsexpress.org/abstract.cfm?URI=oe-15-22-14870

[33] W. P. Grice, A. B. U'Ren, I. A. Walmsley, Eliminating frequency and space-time correlations in multiphoton states, Physical Review A 64 (6) (2001) 063815. doi:10.1103/PhysRevA.64.063815.

[34] P. J. Mosley, J. S. Lundeen, B. J. Smith, I. A. Walmsley, Conditional preparation of single photons using parametric downconversion: a recipe for purity, New Journal of Physics 10 (9) (2008) 093011 (29pp).
URL http://stacks.iop.org/1367-2630/10/093011

[35] O. Cohen, J. S. Lundeen, B. J. Smith, G. Puentes, P. J. Mosley, I. A. Walmsley, Tailored photon-pair generation in optical fibers, Physical Review Letters 102 (12) (2009) 123603. doi:10.1103/PhysRevLett.102.123603.
URL http://link.aps.org/abstract/PRL/v102/e123603

[36] C. Söller, O. Cohen, B. J. Smith, I. A. Walmsley, C. Silberhorn, High-performance single-photon generation with commercial-grade optical fiber, Phys. Rev. A 83 (3) (2011) 031806. doi:10.1103/PhysRevA.83.031806.

[37] L. Cui, X. Li, N. Zhao, Minimizing the frequency correlation of photon pairs in photonic crystal fibers, New Journal of Physics 14 (12) (2012) 123001.
URL http://stacks.iop.org/1367-2630/14/i=12/a=123001

14

[38] M. Yabuno, R. Shimizu, Y. Mitsumori, H. Kosaka, K. Edamatsu, Four-photon quantum interferometry at a telecom wavelength, Phys. Rev. A 86 (2012) 010302. doi:10.1103/PhysRevA.86.010302.
URL http://link.aps.org/doi/10.1103/PhysRevA.86.010302